Carrier Dynamics of Quantum-Dot, Quantum-Dash, and Quantum-Well Semiconductor Optical Amplifiers Operating at 1.55 μm

Aaron J. Zilkie, *Student Member, IEEE*, Joachim Meier, Mo Mojahedi, *Member, IEEE*, Philip J. Poole, Pedro Barrios, Daniel Poitras, Thomas J. Rotter, *Member, IEEE*, Chi Yang, Andreas Stintz, Kevin J. Malloy, *Senior Member, IEEE*, Peter W. E. Smith, *Life Fellow, IEEE*, and J. Stewart Aitchison, *Senior Member, IEEE*

***Abstract*—We assess the influence of the degree of quantum confinement on the carrier recovery times in semiconductor optical amplifiers (SOAs) through an experimental comparative study of three amplifiers, one InAs–InGaAsP–InP quantum dot (0-D), one InAs–InAlGaAs–InP quantum dash (1-D), and one InGaAsP–InGaAsP–InP quantum well (2-D), all of which operate near 1.55-μm wavelengths. The short-lived (around 1 ps) and long-lived (up to 2 ns) amplitude and phase dynamics of the three devices are characterized via heterodyne pump-probe measurements. The quantum-dot device is found to have the shortest long-lived gain recovery ($\sim$80 ps) as well as gain and phase changes indicative of a smaller linewidth enhancement factor, making it the most promising for high-bit-rate applications. The quantum-dot amplifier is also found to have reduced ultrafast transients, due to a lower carrier density in the dots. The quantum-dot gain saturation characteristics and temporal dynamics also provide insight into the nature of the dot energy-level occupancy and the interactions of the dot states with the wetting layer.**

***Index Terms*—Charge carrier lifetime, optical modulation, optical signal processing, quantum dots (QDs), quantum-effect semiconductor devices, quantum wells (QWs), quantum wires, semiconductor optical amplifiers (SOAs), semiconductor switches.**

I. Introduction

THE development of semiconductor quantum dot (QD) lasers and amplifiers has brought about devices which have a zero-dimensional (0-D) or quasi-zero-dimensional density of states, and, theoretically, high differential gains and low threshold current densities. Additionally, the high degree of quantum confinement results in a density of states having discretized energy levels which can significantly modify the bulk carrier dynamics.

Manuscript received March 23, 2007; revised June 18, 2007. This work was supported by the National Science and Engineering Research Council, in part through the research network "Agile All-Photonics Networks."

A. J. Zilkie, M. Mojahedi, P. W. E. Smith, and J. S. Aitchison are with the Edward S. Rogers Sr. Department of Electrical and Computer Engineering, University of Toronto, Toronto, ON M5S 3G4 Canada (e-mail: aaron.zilkie@utoronto.ca).

J. Meier was with the University of Toronto, Toronto, ON M5S 3G4 Canada. He is now with High Q Laser Production GmbH, A-6845 Hohenems, Austria.

P. J. Poole, P. Barrios, and D. Poitras are with the Institute for Microstructural Sciences, National Research Council of Canada, Ottawa, ON K1A 0R6 Canada.

T. J. Rotter, C. Yang, A. Stintz, and K. J. Malloy are with the Center for High Technology Materials, University of New Mexico, Albuquerque, NM 87106 USA.

Color versions of one or more of the figures in this paper are available online at http://ieeexplore.ieee.org.

Digital Object Identifier 10.1109/JQE.2007.904474

QD semiconductor optical amplifiers (SOAs) have recently attracted interest in all-optical signal-processing applications because they have shown potential to recover their gain significantly faster than 2-D multiple-quantum-well (MQW) devices [1]–[3]. QD SOAs operating in the 1.1–1.3-μm wavelength range have recently been reported which have 1–10-ps gain recovery times [4]–[7], whereas MQW or bulk devices typically have gain recovery times of $\sim$100 ps or longer [8]–[11]. One-dimensional quantum dash (QDash) amplifiers are of interest as an alternative to QDs, since they have some dot-like properties and can more easily be made to operate in the important 1.55-μm telecommunications wavelength range, but so far they have been shown to also have longer gain recovery times of $>$100 ps [12].

QD lasers and amplifiers which operate near 1.55 μm have also recently been developed, using a material structure consisting of InAs dots in an InGaAsP matrix on an InP substrate [1], [13]–[17] and are of interest as they could bring the advantages of QDs to the important 1.55-μm wavelength range. However, because these QDs are larger than conventional InAs–GaAs QDs as they form under less strain ($\sim -3\%$ compared with $\sim -6.5\%$ for InAs/GaAs), the strength of the effects of the 0-D confinement and the exact nature of the density of states is not well understood. The carrier dynamics of QD amplifiers, in addition to dictating their high-speed performance in a switching device, provide insight into the energy-level distribution, but to date there have been few attempts to study the carrier dynamics in InAs–InGaAsP–InP QD structures. Here, we study the effects of the 0-D quantum confinement in our InAs–InGaAsP–InP QD SOA by comparing its gain dynamics with a 1.55-μm QDash and QW SOA also based on the InP material system. The long-lived gain recoveries (recoveries lasting up to 2 ns) determine the switching rate, thus a comparison of these lifetimes amongst the three SOAs is of interest. Additionally the short-lived dynamics (on the order of 1 ps), typically resulting form carrier heating (CH) and spectral hole burning (SHB) processes, are compared as they provide insight into the nature of the carrier scattering processes and energy-level distributions and represent undesirable distortions in ultrafast all-optical signal processing at rates approaching 1 THz.

II. Sample Structures

The three samples investigated in this study are p-i-n doped ridge-waveguide diodes, whose structural details are summarized in Table I. The QD SOA is similar to the sample described

TABLE I
SAMPLE STRUCTURES

Sample	Dimensionality	Length [mm]	Ridge Width [μm]	A [cm^2]	Active layer	# of layers	Barrier Layers	Substrate	Growth Method
QD	0	1	2	2×10^{-5}	InAs	5	$In_{0.805}Ga_{0.195}As_{0.405}P_{0.595}$	InP	CBE
QDash	1	1	5	5×10^{-5}	InAs	5	$Al_{0.18}Ga_{0.32}In_{0.5}As$	InP	MBE
QW	2	1	2	2×10^{-5}	$In_{0.805}Ga_{0.195}As_{0.8}P_{0.2}$	5	$In_{0.805}Ga_{0.195}As_{0.405}P_{0.595}$	InP	CBE

in [18], its core consisting of five stacked layers of self-assembled InAs dots, grown in $In_{0.805}Ga_{0.195}As_{0.405}P_{0.595}$ 1.15-μm -bandgap barrier layers and InP cladding layers by chemical beam epitaxy on an InP substrate. It has a ridge width of 2 μm, a length of 1 mm, and it is antireflection (AR)-coated to create a single-pass amplifier. Compared with the structure in [18], it has a slightly reduced active region width and increased p-type dopant concentration to lower the series resistance and improve hole injection, allowing for higher injected currents and more gain. The QD growth conditions were also nominally similar, thus we estimate the dot characteristics to be similar to those in our previous reports, with a planar density of 1.5×10^{10} cm^{-2} and approximate average lateral diameter and height of 25 and 5 nm, respectively, as confirmed by TEM and AFM measurements [19], [20]. We believe the dots are on average slightly larger than those in [18], however, because of the slightly longer observed amplified spontaneous emission (ASE) peak wavelength of 1620 nm (see Fig. 1), which is due to a small increase in the amount of InAs deposited. The QW SOA has been made as similar to the QD SOA as possible, for comparison. It has identical cladding layers and doping, but has a core consisting of five $In_{0.805}Ga_{0.195}As_{0.8}P_{0.2}$ compressively strained QWs in place of the InAs dot layers. The widths of the wells and $In_{0.805}Ga_{0.195}As_{0.405}P_{0.595}$ barriers were adjusted to provide an electroluminescence peak near 1550 nm. The waveguide is 2 μm wide, 1 mm long, and is AR-coated, as with the QD SOA. The QDash sample structure is the same as described in [21] and of the type also reported in [22], [23], consisting of five layers of InAs quantum dashes (highly elongated with axes aligned perpendicular to the waveguide) each embedded in compressively strained $Al_{0.2}Ga_{0.16}In_{0.64}As$ QWs, and separated by tensile-strained 30-nm-thick $Al_{0.18}Ga_{0.32}In_{0.5}As$ barriers. The dimensions of the dashes were estimated to be 300, 25, and 5 nm for the length, width, and height, respectively, and the dash density to be $\sim 1\times10^{10}$ cm^{-2} [23]. This dash-in-a-well layer structure is surrounded with $Al_{0.2}Ga_{0.28}In_{0.52}As$ guiding layers to complete the intrinsic active region, which is then bounded by doped AlInAs upper and lower cladding layers. The entire structure is grown on an InP substrate. The sample has a 5-μm ridge width and is 1 mm in length. The value of A for each sample in Table I is the ridge width multiplied by the sample length and is the cross-sectional areas of the current flow into the active region, neglecting current spreading effects.

III. ELECTRONIC STRUCTURE AND GAIN CHARACTERISTICS

The ASE spectra measured from the three samples are shown together in Fig. 1. The QW and QDash spectra peak at ~1550 nm at maximum bias, and the QD spectrum covers the 1550-nm range and peaks at ~1620 nm at maximum bias. The QW and

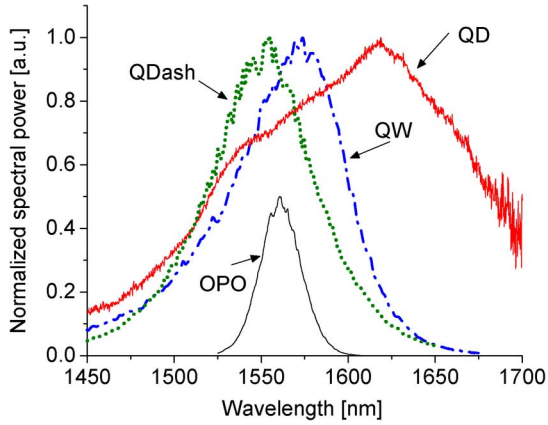

Fig. 1. Normalized ASE spectra of the three SOA samples at maximum bias (QD—thick solid line, FWHM = 164 nm; QDash—dotted line, FWHM = 66 nm; QW—dash-dotted line, FWHM = 72 nm) and the spectrum of the 150 fs OPO pulses (thin solid line, FWHM = 25 nm). The normalized OPO spectrum has been arbitrarily scaled by a factor of 0.5 in the figure.

QDash SOA emission spectra are close to symmetrical with full-widths at half-maximum (FWHM) of 72 and 66 nm, respectively. The QW spectrum derives from the typical 2-D density-of-states (a bulk-like continuum of states modulated by a step function), multiplied by the Fermi–Dirac occupancy probability [24]. In the QDash device, the dashes have lengths which are an order of magnitude greater than their widths, thus the density of states is expected to approximate that of a 1-D quantum wire [25], intermediate between a 2-D continuum and 0-D delta-function density of states. This should lead to a spectrum significantly narrower than a QW, but the emission spectrum of the QDash ensemble is also inhomogeneously broadened by the size variation of the dashes, thus it is close to the QWs in width. The QD has a large ASE FWHM (164 nm), more than double that of the QDash and QW structures. We estimate the QD emission spectrum as one due to a 0-D-like density of states, a series of delta-functions at the dot quantized energies, that are both homogeneously broadened and inhomogeneously broadened by the dot size distribution. Fig. 2 shows the net gain coefficient g_{net} (defined as $T = P_{out}/P_{in} = exp(g_{net}L)$ with the coupling losses accounted for in the transmission P_{out}/P_{in}), measured from the QD SOA versus wavelength for different bias currents. Based on this gain spectrum, we estimate the QD ground state to be at the 1665-nm low-current gain maximum, and the first and second excited states ES1 and ES2 to be at the 1620- and 1580-nm gain peaks, respectively, which reach their maximum and saturate at increasingly higher currents. Based on these three levels, we fit a sum of Gaussians to the ASE spectrum from Fig. 1, as shown in the inset of Fig. 2. A good fit is obtained (solid line) in the 1525–1675-nm wavelength range by

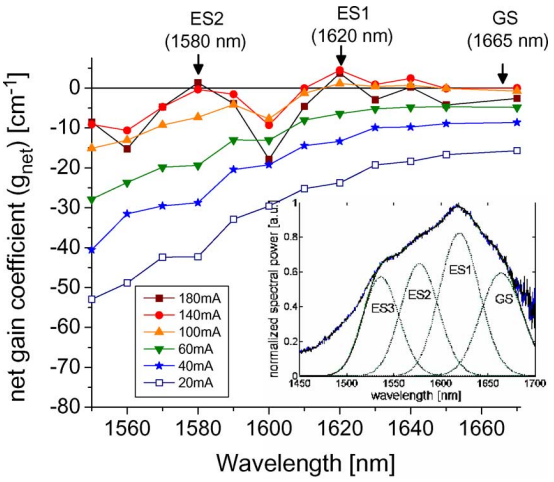

Fig. 2. Net gain coefficient g_{net} versus wavelength for the QD SOA for increasing bias currents. The maxima in the gain curves at high bias correspond to the QD energy levels, indicated by the arrows. Inset: Fit to the ASE spectrum from Fig. 1 (solid line) using a sum of four Gaussian functions (dotted lines), centered at the GS, ES1, and ES2 wavelengths determined from the gain curves, plus an ES3 centered at 1535 nm. An optimum fit was obtained using a FHWM of 49 nm for the Gaussian curves.

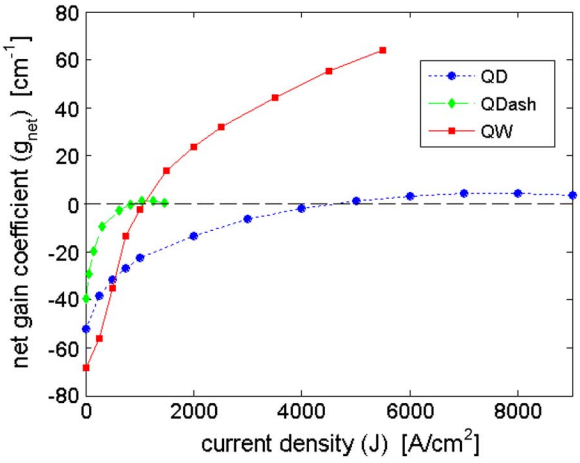

Fig. 3. Net gain coefficient g_{net} versus applied current density, for the three SOAs. The QD gain curve is measured at 1620 nm, and the QDash and QW at 1560 nm.

including a third excited state at $\mathrm{ES3} = 1535$ nm, and, from the fitting, a broadening factor of 49 meV is determined, which is the sum of the inhomogeneous and homogeneous broadening at 300 K. Thus, in our QD structure, the ground state and the excited states have a small energy spacing of ~20 meV, smaller then the broadening of each level. This is consistent with previous reports, on devices made of this long-wavelength QD material system [14], [15], [17] and of low-temperature PL measurements on single InAs–InP QDs [26], which found energy spacings that are less than the inhomogeneous broadening of each level, resulting in a quasi-continuum of levels.

In small highly confined dots (such as more conventional dots formed on GaAs substrates which operate at 1–1.3-μm wavelengths), the energy levels are sufficiently uncoupled from adjacent levels and high-lying wetting layer (WL) continuum levels that the occupancy probability of the levels is not characterized by a Fermi–Dirac distribution. However, because of the quasi-continuum nature of the energy levels in these long-wavelength dots, it is unclear if the same characteristic applies here. We address the question about the nature of the occupancy of the states by comparing the gain saturation characteristics amongst the three devices. Fig. 3 plots the net gain coefficient of the three SOAs versus current density. The current density J for each sample is calculated as the applied bias current divided by the value for A from Table I. The slow gain saturation (low differential gain $dg_{\mathrm{net}}dJ$) and high saturation current density of the QD SOA indicates shallow dots [12], [27] or relatively large dots which can hold larger amounts of carriers before saturating, in contrast to 1–1.3-μm wavelength QDs. Additionally, the gain begins to decrease as the bias is increased past saturation, consistent with the saturation of a Fermi–Dirac-function occupancy of an energy distribution coupled to the WL states, as described in [27]. Further insight into the occupancy of states in the QD device is gained from the study of the temporal dynamics reported in Section IV.

The QW and QD samples have the same waveguide dimensions and thus the same current densities, but the QW achieves a much higher net gain ($g_{\mathrm{net}} > 65\ \mathrm{cm}^{-1}$) compared with the QD ($g_{\mathrm{net}} \leq 4.5\ \mathrm{cm}^{-1}$). Also, the QDash SOA has the highest differential gain $dg_{\mathrm{net}}dJ$ and reaches a maximum net gain of $g_{\mathrm{net}} = 2\ \mathrm{cm}^{-1}$, similar to the QD SOA, but at a much lower current density. Lower gain is typical in QD devices due to their inhomogenously broadened gain spectrum, and a reduced interaction with the optical mode due to fact that the dots are spatially discreet with a relatively low planar density. QD SOAs with net gains of 15 cm^{-1} at 1.3 μm [28] and > 9 cm^{-1} in the 1.45–1.5-μm wavelength window [1] have recently been reported. Although lower gain in a narrow band of wavelengths represents a disadvantage over QW devices in applications such as signal regeneration, the extremely broad gain spectrum represents many advantages for large-tunable-range external cavity lasers [29], short-pulse mode-locked lasers [28], [30], and broadband CW sources [31].

IV. Temporal Dynamics Comparison

A. Experimental Setup

The gain and refractive index dynamics of the SOAs are measured using a heterodyne pump-probe setup, the details of which can be found in [18]. This setup allows for measurement of amplitude and phase dynamics using a pump and probe that are degenerate in both wavelength and polarization. The laser source for the experiments is a Ti:sapphire pumped optical parametric oscillator (OPO) generating nearly Fourier-limited 150-fs pulses at a repetition rate of 76 MHz (spectrum also shown in Fig. 1). The change in the probe amplitude and phase are measured using a radio-frequency (RF) lock-in amplifier to detect the 1.5-MHz beat between the RF-modulated probe and reference beams in a Michelson interferometer at the output of the SOA under test. To improve the phase signal stability and provide for background-free measurements, the pump beam is additionally chopped at 200 Hz, and low-frequency (LF) lock-in amplifiers detect the chopped frequency component in the RF lock-in amplifier amplitude and phase signals. For the

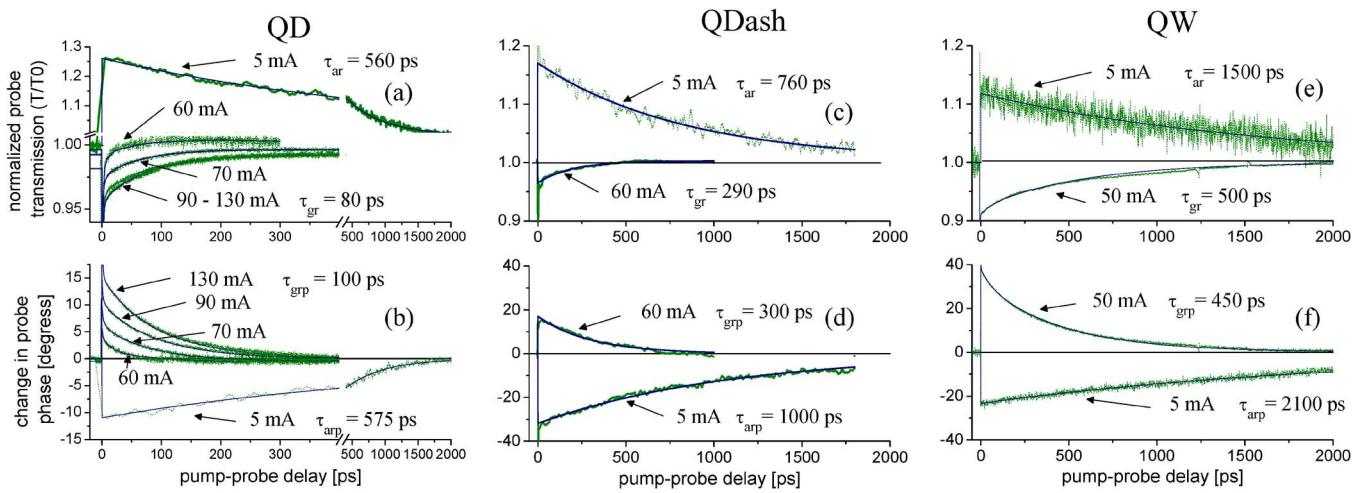

Fig. 4. (a), (c), (e) Long-lived amplitude and (b), (d), (f) phase recoveries over 2 ns for the QD (a), (b), QDash (c), (d), and QW (e), (f) SOAs. Dotted lines are the measured data, and thin solid lines are multi-exponential fits. The bias current in mA and long-lived $1/e$ lifetime in ps of the fit are given for each measured curve.

measurements on the QW and QDash SOAs, the wavelength of the OPO was set to 1560 nm, near the ASE peak of the SOAs, and for the measurements on the QD SOA, to 1620 nm, at the QD ASE and gain peak. For all measurements the polarization state of the pump and probe beams were TE, the pump pulse energies entering the waveguide, accounting for coupling losses, were $\sim$1 pJ, and the probe pulse energies were a factor of 10 lower than the pump energies. The $\sim$1-pJ pump pulse energies were chosen so as to be $\sim$20% of the maximum absorption saturation energy under zero bias, to induce similar saturation effects in all three samples.

B. Long-Lived Dynamics

The recovery of the pump-pulse-induced carrier population back to the equilibrium state is typically of the order of a few hundred picoseconds to a nanosecond in conventional QW or bulk SOAs. Fig. 4 shows the long-lived recoveries measured for the three SOAs, over 2 ns of pump-probe delays. In the absorption regime (low bias currents), the pump pulses induce a net excitation of electron–hole pairs (carriers), causing an increase in probe transmission, and a corresponding decrease in probe phase. The carriers then recombine through spontaneous carrier recombination, giving an exponential decay of the change in probe transmission with $1/e$ lifetime $\tau_{\rm ar}$. In the gain regime (high bias currents), pump-induced stimulated emission reduces the carrier population, resulting in gain bleaching, and a subsequent decrease in probe transmission and increase in probe phase. The gain then recovers exponentially with time constant $\tau_{\rm gr}$ as the carrier population is replenished. The transparency current is the current at which stimulated gain exactly balances stimulated absorption, and there are no net carrier population changes.

In Fig. 4, the recoveries are shown with a multi-exponential fit and associated long-lived $1/e$ lifetime. The transparency currents for the QD, QDash, and QW samples are 40 mA (2000 Acm^{-2}), 23 mA (520 Acm^{-2}), and 15 mA (750 Acm^{-2}) respectively. In the absorption regime the spontaneous carrier recovery times, $\tau_{\rm ar}$ (amplitude traces), and $\tau_{\rm arp}$ (phase traces), are in the range of 0.4–2 ns for all three structures, consistent with previously reported spontaneous recombination rates on the order of 1 ns [4], [32]. The shortest amplitude recovery time, 550 ps, is observed in the QD SOA. The QDash SOA shows an intermediate recovery time of 760 ps, and the QW SOA, which we emphasize has an identical layer structure, composition, and doping to the QD, has a recovery time of 1500 ps, which is almost four times greater than that of the QD. The shorter amplitude recovery times in the QDash and QD SOAs may be caused by carriers in the GS circumventing radiative recombinations by escaping to higher lying WL and continuum states in these more highly confined structures.

The recovery time in the gain regime $\tau_{\rm gr}$ (amplitude traces) and $\tau_{\rm grp}$ (phase traces) is $\sim$80 ps in the QD SOA, $\sim$300 ps in the QDash, and $\sim$500 ps in the QW and is shorter than the corresponding absorption recovery time in all three devices. In the QW SOA, because the QW states are coupled through a continuum of states to the barrier states, the replenishing time is dictated only by the replenishing time of the barrier states. A 500-ps gain recovery is consistent with those typically observed in QW and bulk SOAs with a simple ridge-waveguide or separate-confinement heterostructure (SCH) architecture [9], [11], [32], attributed to Auger-dominated scattering of carriers from the contacts. However, it should be noted that shorter lifetimes have been reported in bulk or QW SOAs with other structures—60 ps in a semi-insulating blocked planar buried heterostructure (SIPBH) MQW structure [10] and as short as 25 ps in small active-area buried waveguide SOAs [33], [34]. The $\sim$300-ps gain recovery time observed in our QDash SOA is in general agreement with the 100–200-ps gain recoveries found for QDash SOAs in [12] and [25]. The $\sim$80-ps gain recovery time in the QD is also similar to the recovery time found for the InAs–InGaAs–GaAs QDs in [12]. We note that no significant dependency of the recovery times on bias current was observed.

The long-lived gain recovery time is six times faster in the QD SOA than in the QW, confirming that 3-D quantum confinement leads to a shorter gain recovery time, and indicating that the QD SOA is the most promising for ultrafast signal processing. Physically, the QD energy states are coupled to the higher lying continuum levels in the WL [27], and under gain-regime applied

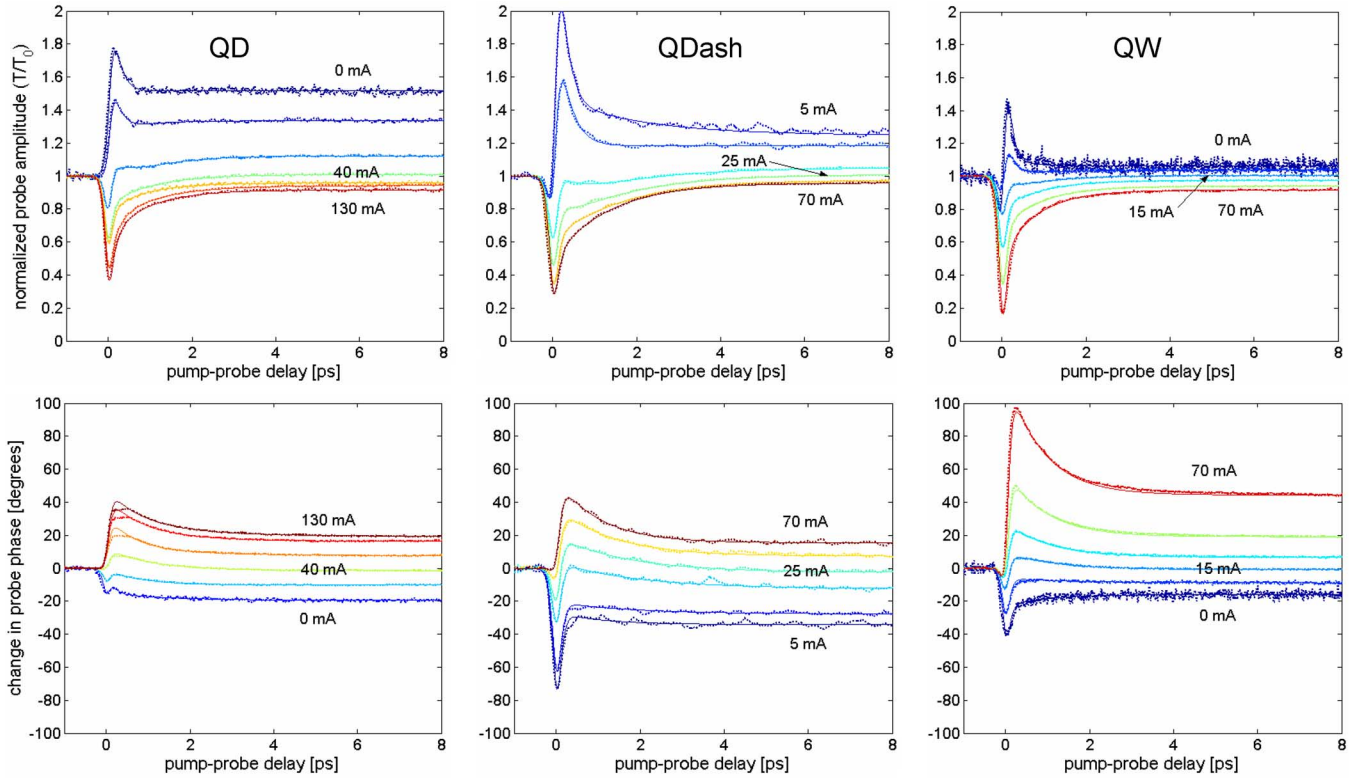

Fig. 5. Ultrafast amplitude (top row) and phase (bottom row) dynamics of the QD (left column), QDash (middle column), and QW (right column) SOAs, measured over 8 ps, for varying bias currents. Dotted lines show the measured data and thin solid lines show the double-exponential fits to the data. The labeled bias currents are the minimum applied, transparency, and maximum applied currents.

biases, carriers occupy not only the dot states, but also some of the WL states. The WL carriers act as a reservoir feeding the dot states through fast phonon-assisted carrier capture processes [4], and the gain recovery time is shorter because the carrier replenishing is due to a combination of WL carrier replenishing and faster dot capture processes. The QD phase dynamics in Fig. 4(d) show a complete phase recovery within ∼100 ps, indicating that the entire carrier population returns to equilibrium in this time-frame. The QDash SOA gain recovery time is also shorter than that of the QW, indicating that the wire-like quantum confinement, combined with the presence of a WL and a finite dash volume similar to as in QDs, also results in a shortened gain recovery lifetime. Our findings support the theoretical conclusions in [35] and experimental evidence in [36] that dot capture and WL replenishing times still limit QD device gain recovery lifetimes to values longer than the subpicosecond lifetimes of SHB recoveries [4], [6], [7].

Lastly, we note that weak intermediate-lifetime exponential decay terms are observed in the absorption and gain recoveries for all three SOAs [as can be seen, for example, in the 60-mA trace in Fig. 4(a)]. These dynamics have a ∼5-ps lifetime in the QD, a ∼20-ps lifetime in the QDash and QW, and have a magnitude of $a \approx -0.015$ to -0.02 ($\sim 3\times$ less than $a_{\rm cr}$ at max gain and $> 10\times$ less than $a_{\rm CH}$) in all three samples. This intermediate dynamic is always negative and is present for all bias currents including around transparency, thus it behaves like a weak secondary longer lived carrier heating response. Longer lived carrier heating dynamics of this nature have not been reported in previous studies and these dynamics deserve further investigation. This intermediate dynamic also explains the short 15-ps gain recovery time found in our earlier QD sample in [18]. Since the maximum current that could be applied was 60 mA, the gain was still sufficiently weak that the intermediate dynamic dominated, and the full gain recovery lifetime could not be observed.

C. Short-Lived Dynamics

Fig. 5 shows the ultrafast dynamics of the three SOAs measured for varying bias currents over a range of 8 ps. The top row shows the amplitude responses and the bottom row the phase. The absorption and gain regimes are identifiable by the direction of the step changes, which correspond to the long-lived components presented in Section IV-B. Gain saturation occurrs at a bias current of 130 mA (6500 A/cm^2) in the QD SOA, 70 mA (1450 A/cm^2) in the QDash, and the maximum bias applied to the QW SOA was 70 mA (3500 A/cm^2). The transparency currents, the currents at which the step change is zero, are also indicated in the figure. Good fits (solid lines in Fig. 5) to the traces from all three SOAs were achieved by fitting with a double-exponential impulse response function as described in [18] and convolving with a laser pulse cross-correlation signal corresponding to our 150-fs Gaussian OPO pulses. The double-exponential model contains terms which account for spectral hole burning (SHB), carrier heating (CH), as well as the instantaneous two-photon absorption (TPA) response.

Fig. 6 plots the magnitudes of the step changes, $a_{\rm cr}$ (amplitude changes), and $a_{\rm crp}$ (phase changes) measured in each of the three SOAs, versus bias current normalized to the transparency current $(I/I_{\rm tr})$. The magnitudes of the step changes correspond

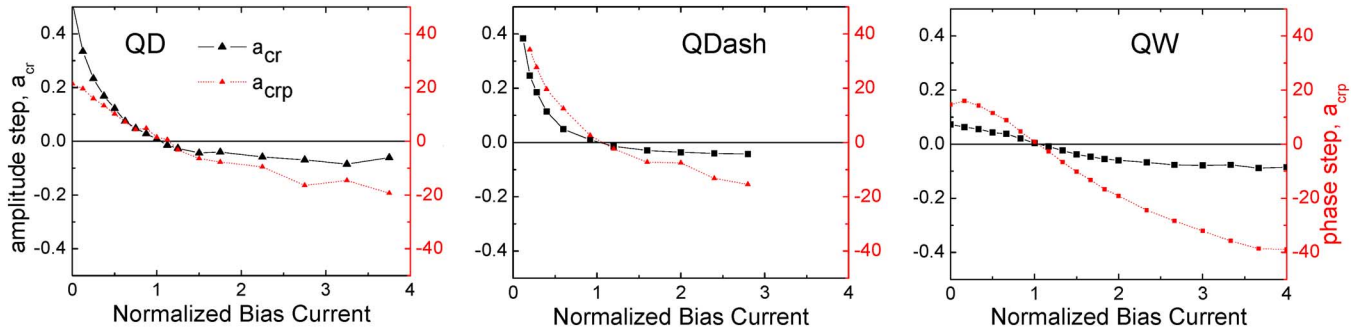

Fig. 6. Magnitudes of the step changes, $a_{\rm cr}$ (amplitude—left axis of the three plots) and $a_{\rm crp}$ (phase—right axis of the three plots), in the fits to the curves in Fig. 5, versus normalized bias current $I/I_{\rm tr}$.

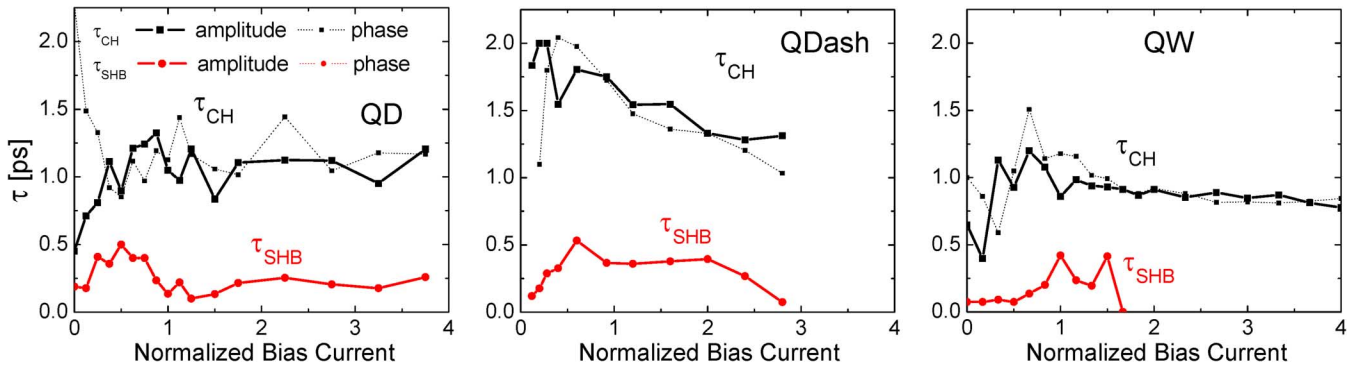

Fig. 7. $1/e$ lifetimes of the CH ($\tau_{\rm CH}$) and SHB ($\tau_{\rm SHB}$) components in the fits to the amplitude (solid curves) and phase (dotted curves) curves in Fig. 5 versus normalized bias current. No SHB dynamic was observed in the phase traces, which is consistent with hole burning symmetric about the center frequency [6], [32].

to the magnitudes of the long-lived recoveries shown in Fig. 4 and represent the magnitudes of the amplitude saturation and phase change achievable in the three SOAs for a 1-pJ input pulse energy. In the QD SOA, the trend in $a_{\rm cr}$ shows that the changes in gain saturate at $I/I_{\rm tr} = 3.25$ ($I = 130$ mA), the same current at which the gain saturates in Fig. 3. However, the magnitude of the phase change continues to increase past 130 mA. Thus, when the ground state gain is saturated at high biases, changes in the carrier population still increasingly effect the excited state and WL state populations to some extent. The similarity of the slow gain saturation and lack of phase saturation to the QW $a_{\rm cr}$ trend further points to a Fermi–Dirac distribution in the QD sample which couples the dot and WL states. We also observe that the maximum gain and absorption changes are largest in the QD SOA and smallest in the QW SOA, while at the same time the phase changes are smallest in the QD SOA and largest in the QW SOA. At low bias currents, a four-times-smaller absorption saturation in the QW SOA compared with the QD results in a relatively equal phase change, while at high bias currents an equal gain change induces twice the phase change in the QW. Similarly, smaller gain changes in the QDash SOA compared with those of the QD result in equal or slightly greater phase changes at all bias currents. Thus, the QD SOA has the lowest linewidth enhancement factor, at all bias currents, suggesting it is the best choice in high-bit-rate applications for producing minimum patterning effects. We again attribute this to the effects of the 3-D quantum confinement in the QDs. A larger absorption and gain saturation is a result of a stronger gain change as a function of carrier density at the excitation wavelength due to a more delta-function-like density of states. This is supported by the corresponding phase changes, which are related, by the Kramers–Kronig relations [6], [32], to the integral of the gain change over all energies. A weak phase change implies a more symmetrical gain depletion versus energy, as well as a dot carrier distribution which is more weakly coupled to higher lying (WL) states. We note, however, that the linewidth enhancement factor is expected to vary significantly over the gain spectrum of a QD SOA, due to the effect of excited states. A more detailed study of the linewidth enhancement factor will be reported in a future work. Lastly, the intermediate behavior of the QDash amplitude and phase trends again demonstrates the intermediate nature of the effects of the 2-D confinement in the QDash sample.

The lifetimes and trends of the ultrafast CH and SHB components provide additional insight into the physics of the carrier interactions and the effects of the quantum confinement on the carrier distributions. Fig. 7 plots the $1/e$ lifetimes of the CH ($\tau_{\rm CH}$) and SHB ($\tau_{\rm SHB}$) recoveries found in the three SOAs versus $\rm I/I_{tr}$, and Fig. 8 plots the associated magnitudes of the CH dynamic, $a_{\rm CH}$. We find CH and SHB lifetimes nominally similar amongst all three SOAs and similar amongst the amplitude and phase traces, with $\tau_{\rm CH} \approx$1–2 ps and $\tau_{\rm SHB} \approx$0.1–0.5 ps. This indicates the same SHB and CH physical mechanisms (see [18] for details) are present in all three structures, independent of the degree of quantum confinement.

In the QDash and QW devices, $\tau_{\rm CH}$ shows a bias dependence. We suggest that this is due to a changing of the dominant CH process between free-carrier absorption (FCA) heating and stimulated transitions (ST) heating. FCA transitions excite

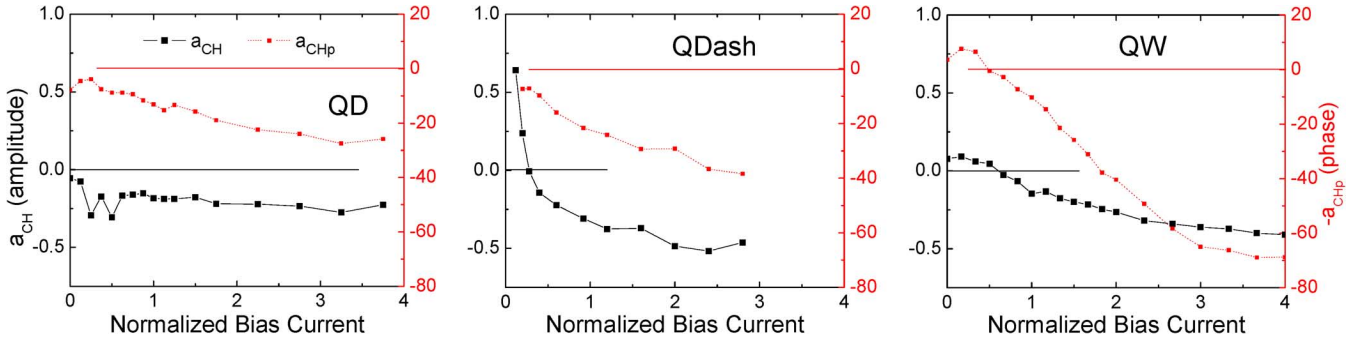

Fig. 8. Magnitudes of the CH component, a_{CH} (amplitude—solid curves, left axes) and $a_{\mathrm{CH_P}}$ (phase—dotted curves, right axes), in the exponential fits to the curves in Fig. 5 versus normalized bias current.

carriers from near the bottom of the conduction band to states higher up in the conduction band, whereas stimulated transitions simply create carriers in (absorption regime) or remove carriers from (gain regime) the states near the bottom of the conduction band. Thus, FCA heating has a longer recovery time, ∼1.5 ps, compared with ST recoveries, ∼0.8 ps [18], [37]. Also, at transparency, stimulated transitions are zero and only FCA-heating is present. In the QW SOA, τ_{CH} peaks at a value of 1–1.5 ps at transparency, indicating a 1–1.5 ps FCA-heating recovery. As the bias is increased, τ_{CH} decreases and approaches ∼0.8 ps, indicating that ST heating is taking over as the dominant process at high biases. Furthermore, ST heating can result in carrier cooling (a positive a_{CH}) at low bias currents [18], [37]. The carrier cooling observed in Fig. 8 indicates that ST heating is also dominant at low bias currents in the QDash and QW SOAs. The presence of carrier cooling implies an average carrier energy that is greater than the pump-probe photon energy at low biases, which could be a result of a density of states which extends to higher energies in the cases of 1-D and 2-D confinement. However, we believe the observation of carrier cooling is dependent on where the pump photon energies are with respect to the gain spectrum at low bias (i.e., if they are above, near, or below the gain peak), particularly in QD devices which have multiple gain maxima. Carrier cooling was observed at low bias in measurements on our earlier QD device [18], where the pump photons were at energies above those of the gain maximum, whereas, in the measurements on the QD sample reported here, carrier cooling is not observed when the pump photons energies are very near the gain maximum. Further measurements to obtain the sign of the carrier heating dynamic over a wide range of wavelengths within the gain spectrum are needed to better reveal the dependence of carrier cooling on photon energy. Lastly, we observe that the FCA carrier heating lifetime in the QDash SOA at transparency, τ_{CH} =1.5–2 ps, is larger than in the QD and QW SOA. We theorize that this is due to the different material in the QDash active region, InGaAlAs, as opposed to InGaAsP in the QD and QW structures. This is consistent with the 1.6-ps dynamic observed in InAs–InGaAlAs QDashes in [12].

In the QD SOA, we note that τ_{CH} is constant at its transparency value of ≈1 ps. We thus conclude that CH in the QD is dominated by FCA heating at all bias currents above $I/I_{tr} = 0.5$. This observation is in contrast to the CH responses seen in previous studies of 1.1- and 1.3-μm QDs [4], [6], respectively, which attributed weak CH dynamics to a lack of FCA. This again corroborates that our QDs are larger, contain more energy states, and have a more Fermi-Dirac-like occupancy probability. The CH magnitudes in the QD sample observed in Fig. 8 are weaker than in the QDash and QW samples however, because of the lower carrier density and lower gain. The magnitude of CH in the QD phase dynamics is also much weaker than in the QW, implying a heated distribution that is less changed over all energies, supporting the finding iearlier in this section that the QD carrier distribution is less coupled to higher energies. The much weaker CH in the phase dynamics in the QDs again represents an advantage over QWs in ultrafast signal processing and high-data-rate applications, where large transients are undesirable, although, at the same time, a low overall phase change is a disadvantage for phase-based switching. The strong CH phase transients consistently observed in QW SOAs could ultimately represent a limit to the high-speed performance of QW devices if they are to be used for ultrafast applications.

Lastly, SHB lifetimes of τ_{SHB} ≈0.1–0.5 ps are consistent with expected inter-level carrier–carrier scattering lifetimes amongst the energy states within the quantum-confined regions [5], [32], [38]. Carrier–carrier scattering times were found to shorten with increasing carrier density in [32], thus, in the QW, a decreasing τ_{SHB} which approaches zero (indistinguishable from zero in our 150-fs resolution measurements) for high biases indicates a higher carrier density than in the QDash and QD at high biases.

V. Conclusion

We have studied and compared the amplitude and phase recovery dynamics in three SOAs with different dimensionalities—a QW and QD InAs–InGaAsP–InP SOA with identical barrier and cladding layer structures, and an InAs–InAlGaAs–InP QDash SOA, each operating near 1.55 μm and grown on an InP substrate—in order to assess the influence of the degree of quantum confinement on an SOA's carrier dynamics and high-speed performance. The QD SOA has a smaller maximum gain and a smaller phase change compared with the QW, but it has a much broader gain bandwidth, making it superior to QW SOAs in applications such as large-tunable-range external cavity lasers, short-pulse mode-locked lasers, and broadband CW sources. Comparing the long-lived gain recoveries of the three SOAs showed that the lower the dimensionality in the active region, the shorter the gain recovery time. The QD SOA gain recovery $1/e$ lifetime was ∼80 ps,

which is six times faster than in the QW and four times faster than in the QDash. Thus, our QD SOA is capable of the fastest switching rates in all-optical signal processing applications. The QDash SOA gain recovery time and short-lived amplitude and phase dynamic trends were between those of the QD and QW, indicating the intermediate nature of the performance of 1-D devices. We also found ultrafast CH and SHB dynamics nominally similar in all three SOAs, with carrier heating recovery lifetimes of 1–2 ps and $\sim$0.8 ps, attributed to FCA-induced heating and stimulated-transition-induced heating, respectively. Despite the theoretically 0-D nature of QDs, the gain saturation behavior, phase dynamics, and carrier heating effects in our QD SOA indicate a Fermi–Dirac occupancy probability with coupled dot and WL states and a lower carrier density, due to larger dots with more states, as well as a gain recovery time limited by the dot-WL carrier interactions. However, larger gain changes with smaller associated phase changes still imply a more symmetrical delta-function-like 0-D density of states as compared with the QDash and QW sturctures, giving the QD SOA a lower linewidth enhancement factor. Also, weaker CH effects in our 1.55-μm QD structure confirms it has suppressed ultrafast transients, as with 1.1- and 1.3-μm dots, which is an additional advantage for high-data-rate applications.

ACKNOWLEDGMENT

One of the authors, A. J. Zilkie, would like to acknowledge M. Y. Xu and S. B. Kuntze for helpful discussions.

REFERENCES

[1] M. Sugawara, N. Hatori, M. Ishida, H. Ebe, Y. Arakawa, T. Akiyama, K. Otsubo, T. Yamamoto, and Y. Nakata, "Recent progress in self-assembled quantum-dot optical devices for optical telecommunication: Temperature-insensitive 10 Gbs(-1) directly modulated lasers and 40 Gbs(-1) signal-regenerative amplifiers," *J. Phys. D., Appl. Phys.*, vol. 38, pp. 2126–2134, Jul. 2005.

[2] T. Akiyama, N. Hatori, Y. Nakata, H. Ebe, and M. Sugawara, "Pattern-effect-free amplification and cross-gain modulation achieved by using ultrafast gain nonlinearity in quantum-dot semiconductor optical amplifiers," *Phys. Status. Solidi B*, vol. 238, pp. 301–304, Jul. 2003.

[3] A. V. Uskov, E. P. O'Reilly, R. J. Manning, R. P. Webb, D. Cotter, M. Laemmlin, N. N. Ledentsov, and D. Bimberg, "On ultrafast optical switching based on quantum-dot semiconductor optical amplifiers in nonlinear interferometers," *IEEE Photon. Technol. Lett.*, vol. 16, no. 4, pp. 1265–1267, May 2004.

[4] P. Borri, S. Schneider, W. Langbein, U. Woggon, A. E. Zhukov, V. M. Ustinov, N. N. Ledentsov, Z. I. Alferov, D. Ouyang, and D. Bimberg, "Ultrafast carrier dynamics and dephasing in InAs quantum-dot amplifiers emitting near 1.3- μm-wavelength at room temperature," *Appl. Phys. Lett.*, vol. 79, pp. 2633–2635, Oct. 2001.

[5] M. van der Poel, E. Gehrig, O. Hess, D. Birkedal, and J. M. Hvam, "Ultrafast gain dynamics in quantum-dot amplifiers: Theoretical analysis and experimental investigations," *IEEE J. Quantum Electron.*, vol. 41, no. 9, pp. 1115–1123, Sep. 2005.

[6] P. Borri, W. Langbein, J. M. Hvam, F. Heinrichsdorff, M. H. Mao, and D. Bimberg, "Spectral hole-burning and carrier-heating dynamics in InGaAs quantum-dot amplifiers," *IEEE J. Sel. Topics Quantum Electron.*, vol. 6, no. 3, pp. 544–551, May–Jun 2000.

[7] P. Borri, S. Schneider, W. Langbein, and D. Bimberg, "Ultrafast carrier dynamics in InGaAs quantum dot materials and devices," *J. Opt. A, Pure. Appl. Opt.*, vol. 8, pp. S33–S46, Apr. 2006.

[8] K. L. Hall, J. Mark, E. P. Ippen, and G. Eisenstein, "Femtosecond gain dynamics in ingaasp optical amplifiers," *Appl. Phys. Lett.*, vol. 56, pp. 1740–1742, Apr. 1990.

[9] G. Eisenstein, J. M. Wiesenfeld, M. Wegener, G. Sucha, D. S. Chemla, S. Weiss, G. Raybon, and U. Koren, "Ultrafast gain dynamics in 1.5 mu-m multiple quantum-well optical amplifiers," *Appl. Phys. Lett.*, vol. 58, pp. 158–160, Jan. 1991.

[10] K. L. Hall, Y. Lai, E. P. Ippen, G. Eisenstein, and U. Koren, "Femtosecond gain dynamics and saturation behavior in InGaAsP multiple quantum-well optical amplifiers," *Appl. Phys. Lett.*, vol. 57, pp. 2888–2890, Dec. 1990.

[11] S. Weiss, J. M. Wiesenfeld, D. S. Chemla, G. Raybon, G. Sucha, M. Wegener, G. Eisenstein, C. A. Burrus, A. G. Dentai, U. Koren, B. I. Miller, H. Temkin, R. A. Logan, and T. Tanbunek, "Carrier capture times in 1.5 μm multiple quantum-well optical amplifiers," *Appl. Phys. Lett.*, vol. 60, pp. 9–11, Jan. 1992.

[12] M. van der Poel, J. Mork, A. Somers, A. Forchel, J. P. Reithmaier, and G. Eisenstein, "Ultrafast gain and index dynamics of quantum dash structures emitting at 1.55 μm," *Appl. Phys. Lett.*, vol. 89, pp. 081102-1–081102-3, Aug. 2006.

[13] C. N. Allen, P. J. Poole, P. Barrios, P. Marshall, G. Pakulski, S. Raymond, and S. Fafard, "External cavity quantum dot tunable laser through 1.55 μm," *Physica E*, vol. 26, pp. 372–376, Feb. 2005.

[14] S. Anantathanasarn, R. Notzel, P. J. van Veldhoven, F. W. M. van Otten, Y. Barbarin, G. Servanton, T. de Vries, E. Smalbrugge, E. J. Geluk, T. J. Eijkemans, E. A. J. M. Bente, Y. S. Oei, M. K. Smit, and J. H. Wolter, "Lasing of wavelength-tunable (1.55 μm region) InAs/InGaAsP/InP (100) quantum dots grown by metal organic vapor-phase epitaxy," *Appl. Phys. Lett.*, vol. 89, pp. 073115-1–073115-3, Aug. 2006.

[15] Y. M. Qiu, D. Uhl, R. Chacon, and R. Q. Yang, "Lasing characteristics of InAs quantum-dot lasers on (001) InP substrate," *Appl. Phys. Lett.*, vol. 83, pp. 1704–1706, Sep. 2003.

[16] H. D. Kim, W. G. Jeong, J. H. Lee, J. S. Yim, D. Lee, R. Stevenson, P. D. Dapkus, J. W. Jang, and S. H. Pyun, "Continuous-wave operation of 1.5 μm InGaAs/InGaAsP/InP quantum dot lasers at room temperature," *Appl. Phys. Lett.*, vol. 87, pp. 083110-1–083110-3, Aug. 2005.

[17] P. Caroff, C. Paranthoen, C. Platz, O. Dehaese, H. Folliot, N. Bertru, C. Labbe, R. Piron, E. Homeyer, A. Le Corre, and S. Loualiche, "High-gain and low-threshold InAs quantum-dot lasers on InP," *Appl. Phys. Lett.*, vol. 87, pp. 243107-1–243107-3, Dec. 2005.

[18] A. J. Zilkie, J. Meier, P. W. E. Smith, M. Mojahedi, J. S. Aitchison, P. J. Poole, C. N. Allen, P. Barrios, and D. Poitras, "Femtosecond gain and index dynamics in an InAs/InGaAsP quantum dot amplifier operating at 1.55 μm," *Opt. Exp.*, vol. 14, pp. 11453–11459, Nov. 2006.

[19] C. N. Allen, P. J. Poole, P. Marshall, J. Fraser, S. Raymond, and S. Fafard, "InAs self-assembled quantum-dot lasers grown on (100) InP," *Appl. Phys. Lett.*, vol. 80, pp. 3629–3631, May 2002.

[20] C. N. Allen, "Points quantiques sur substrat d'InP: Plate-forme pour des composantes optoelectroniques accordables," Ph.D. dissertation, Dept. of Physics, Univ. of Ottawa, Ottawa, ON, Canada, 2005.

[21] J. Meier, A. J. Zilkie, M. Mojahedi, J. S. Aitchison, R. H. Wang, T. J. Rotter, C. Yang, A. Stintz, and K. J. Malloy, "Gain recovery dynamics in InAs-quantum dash optical amplifiers operating at 1550 nm," in *Proc. Conf. Lasers and Electro-Optics (CLEO) 2006*, Long Beach, CA, 2006, p. CThGG4.

[22] B. Leesti, A. J. Zilkie, J. S. Aitchison, M. Mojahedi, R. H. Wang, T. J. Rotter, C. Yang, A. Stintz, and K. J. Malloy, "Broad-band wavelength up-conversion of picosecond pulses via four-wave mixing in a quantum-dash waveguide," *IEEE Photon. Technol. Lett.*, vol. 17, no. 5, pp. 1046–1048, May 2005.

[23] R. H. Wang, A. Stintz, P. M. Varangis, T. C. Newell, H. Li, K. J. Malloy, and L. F. Lester, "Room-temperature operation of InAs quantum-dash lasers on InP (001)," *IEEE Photon. Technol. Lett.*, vol. 13, no. 8, pp. 767–769, Aug. 2001.

[24] B. E. A. Saleh and M. C. Teich, *Fundamentals of Photonics*, 2nd ed. Hoboken, NJ: Wiley, 2007, pp. 654–672.

[25] J. P. Reithmaier, A. Somers, S. Deubert, R. Schwertberger, W. Kaiser, A. Forchel, M. Calligaro, P. Resneau, O. Parillaud, S. Bansropun, M. Krakowski, R. Alizon, D. Hadass, A. Bilenca, H. Dery, V. Mikhelashvili, G. Eisenstein, M. Gioannini, I. Montrosset, T. W. Berg, M. van der Poel, J. Mork, and B. Tromborg, "InP based lasers and optical amplifiers with wire-/dot-like active regions," *J. Phys. D, Appl. Phys.*, vol. 38, pp. 2088–2102, Jul. 2005.

[26] D. Chithrani, R. L. Williams, J. Lefebvre, P. J. Poole, and G. C. Aers, "Optical spectroscopy of single, site-selected, InAs/InP self-assembled quantum dots," *Appl. Phys. Lett.*, vol. 84, pp. 978–980, Feb. 2004.

[27] D. R. Matthews, H. D. Summers, P. M. Smowton, and M. Hopkinson, "Experimental investigation of the effect of wetting-layer states on the gain-current characteristic of quantum-dot lasers," *Appl. Phys. Lett.*, vol. 81, pp. 4904–4906, Dec. 2002.

[28] M. Laemmlin, G. Fiol, M. Kuntz, F. Hopfer, A. Mutig, N. N. Ledentsov, A. R. Kovsh, C. Schubert, A. Jacob, A. Umbach, and D. Bimberg, "Quantum dot based photonic devices at 1.3 μm: Direct modulation, mode-locking, SOAs and VCSELs," *Phys. Stat. Sol. (C)*, vol. 3, pp. 391–394, 2006.

[29] G. Ortner, C. N. Allen, C. Dion, P. Barrios, D. Poitras, D. Dalacu, G. Pakulski, J. Lapointe, P. J. Poole, W. Render, and S. Raymond, "External cavity InAs/InP quantum dot laser with a tuning range of 166 nm," *Appl. Phys. Lett.*, vol. 88, pp. 121119-1–121119-3, Mar. 2006.
[30] A. R. Rae, M. G. Thompson, R. V. Penty, I. H. White, A. R. Kovsh, S. S. Mikhrin, D. A. Livshits, and I. L. Krestnikov, "Harmonic mode-locking of a quantum-dot laser diode," in *Proc. IEEE LEOS 19th Annu. Meet.*, Montreal, QC, Canada, 2006, p. ThR5.
[31] H. S. Djie, B. S. Ooi, X. M. Fang, Y. Wu, J. M. Fastenau, W. K. Liu, and M. Hopkinson, "Room-temperature broadband emission of an InGaAs/GaAs quantum dots laser," *Opt. Lett.*, vol. 32, pp. 44–46, Jan. 2007.
[32] K. L. Hall, G. Lenz, A. M. Darwish, and E. P. Ippen, "Subpicosecond gain and index nonlinearities in InGaAsP diode-lasers," *Opt. Commun.*, vol. 111, pp. 589–612, Oct. 1994.
[33] R. Giller, R. J. Manning, and D. Cotter, "Gain and phase recovery of optically excited semiconductor optical amplifiers," *IEEE Photon. Technol. Lett.*, vol. 18, no. 3, pp. 1061–1063, May–Jun. 2006.
[34] R. J. Manning, X. Yang, R. P. Webb, R. Giller, F. C. G. Gunning, and A. D. Ellis, "The 'turbo-switch'—A novel technique to increase the high-speed response of SOAs for wavelength conversion," in *Proc. Conf. Opt. Fiber Commun. (OFC)*, Anaheim, CA, 2006, p. OWS8.
[35] T. W. Berg, S. Bischoff, I. Magnusdottir, and J. Mork, "Ultrafast gain recovery and modulation limitations in self-assembled quantum-dot devices," *IEEE Photon. Technol. Lett.*, vol. 13, no. 6, pp. 541–543, Jun. 2001.
[36] D. R. Matthews, H. D. Summers, P. M. Smowton, P. Blood, P. Rees, and M. Hopkinson, "Dynamics of the wetting-layer-quantum-dot interaction in InGaAs self-assembled systems," *IEEE J. Quantum Electron.*, vol. 41, no. 3, pp. 344–350, Mar. 2005.
[37] C. K. Sun, H. K. Choi, C. A. Wang, and J. G. Fujimoto, "Studies of carrier heating in InGaAs/AlGaAs strained-layer quantum-well diode-lasers using a multiple wavelength pump probe technique," *Appl. Phys. Lett.*, vol. 62, pp. 747–749, Feb. 1993.
[38] S. Schneider, P. Borri, W. Langbein, U. Woggon, R. L. Sellin, D. Ouyang, and D. Bimberg, "Excited-state gain dynamics in InGaAs quantum-dot amplifiers," *IEEE Photon. Technol. Lett.*, vol. 17, no. 10, pp. 2014–2016, Oct. 2005.

Aaron J. Zilkie (S'97) was born in Winnipeg, MB, Canada, in 1978. He received the B.Sc. degree in electrical engineering from the University of Manitoba, Winnipeg, MB, Canada in 2001, and the M.A.Sc. degree in electrical and computer engineering from the University of Toronto, Toronto, ON, Canada, where he is currently working toward the Ph.D. degree in electrical and computer engineering.

He interned at Nortel Networks, Ottawa, from 1999 to 2000 in the optical networks division before beginning his graduate work. His current research interests include semiconductor quantum dot (QD) devices, SOAs for all-optical switching, and nonlinear processes in semiconductor materials and their applications.

Mr. Zilkie is a student member of the Optical Society of America.

Joachim Meier received the degree of Dipl.-Ing. (FH) in electrical engineering from the University of Applied Science, Regensburg, Germany, in 1998, and the M.S. and Ph.D degrees in optics from the College of Optics, University of Central Florida, Orlando, in 2000 and 2004, respectively.

He is currently with High Q Laser Production, Hohenems, Austria.

Mo Mojahedi received the Ph.D. degree from the Center for High Technology Materials (CHTM), University of New Mexico (UNM), Albuquerque, in 1999.

Immediately after completing his doctoral work, he joined CHTM as a Research Assistant Professor. In August 2001, he joined the Faculty of the Electrical and Computer Engineering, University of Toronto, Toronto, ON, Canada. His research interests span a wide range of topics which includes matter–wave interactions, abnormal velocities, metamaterials, photonic crystals, dispersion engineering, quantum-dot and -well lasers, fundamental electromagnetic theory, and macro and nanoscale microwave and photonic devices.

Dr. Mojahedi was the recipient of the Popejoy Award for the Outstanding Doctoral Dissertation in Physics and Engineering at UNM for the years 1997–2000.

Philip J. Poole received the B.Sc. degree in physics and the Ph.D. degree from Imperial College, University of London, London, U.K., in 1989 and 1993, respectively.

He joined the National Research Council, Ottawa, ON, Canada, in 1993, where he was involved with the optical properties of semiconductors concentrating on the application of quantum-well intermixing to optical device integration. In 1996, he switched to the growth of InP-based semiconductor structures using chemical beam epitaxy for both optoelectronic devices and fundamental studies. These include the study of the growth of self-assembled quantum dots and selective-area epitaxy for the creation of novel nanostructures.

Pedro Barrios received the B.Sc. degree in electronic engineering from the IUPFAN, Venezuela, in 1989, and the the M.S. and Ph.D. degrees in electrical engineering from the University of Pittsburgh, Pittsburgh, PA, in 1993 and 1997, respectively.

He was a Post-Doctoral Fellow with the NanoFAB Center, Texas A&M University, College Station, during 1998–1999 and with the Electrical Engineering Department of the University of Notre Dame, Notre Dame, IN, from 1999 to 2000. Currently, he is with the Nanofabrication Group, Institute for Microstructural Sciences, National Research Council of Canada, Ottawa, ON. He is currently pursuing research in fabrication of electronic and optoelectronic devices on Si and III-V semiconductors. He has also investigated the oxidation of III-V native oxides (AlGaAs and InAlP) with a focus on materials, fabrication, and characterization of MOS and HEMT devices, as well as research in electronic materials characterization and development of thin films and nanostructure devices on Si.

Dr. Barrios is a member of the Materials Research Society.

Daniel Poitras received the Ph.D. degree from École Polytechnique de Montréal, Montreal, QC, Canada, in 2000, where he worked on plasma-deposited inhomogeneous optical coatings.

He is a Research Officer with the National Research Council of Canada, Ottawa, ON. His interests cover all the research aspects of optical coatings (new applications, theory, design, fabrication, and characterization).

Thomas J. Rotter (M'06) received the M.S. degree from the Westphaelische Wilhelms-Universitaet Muenster, Muenster, Germany, in physics in 1997. He is currently working toward the Ph.D. degree at the University of New Mexico (UNM), Albuquerque.

In 1998, he joined the Center for High Tech Materials, UNM. His research work includes ultrashort pulse lasers, molecular beam epitaxy growth of semiconductor materials, semiconductor lasers and self-assembled quantum nanostructures.

Mr. Rotter is a member of the Optical Society of America.

Chi Yang was born in Henan, China, in 1975. He received the B.E. degree in optical engineering from Zhejiang University, Hangzhou, China, in 1996, and the M.S. degree in optics from Shanghai Institute of Optics and Fine Mechanics, Chinese Academy of Sciences (CAS), Shanghai, China, in 1999. He is currently working toward the Ph.D. degree in electrical engineering at the University of New Mexico, Albuquerque.

His research interests include quantum-dot vertical-cavity surface-emitting lasers, strained quantum-well lasers, and high-power lasers.

Andreas Stintz was born in Merseburg, Germany, in 1964. He received the Ph.D. degree in physics from the University of New Mexico (UNM), Albuquerque, in 1993. The subject of his dissertation was field desorption phenomena.

From 1994 to 1995, he was a Postdoctoral Fellow with the Department of Physics and Astronomy, UNM, where he investigated the singlet D resonance in the ion. In 1996, he joined the Center for High Technology Materials, UNM, and became involved in crystal growth for III-V semiconductors by molecular beam epitaxy. His research includes high-power quantum-well lasers, quantum-dot lasers and detectors, saturable absorbers, and crystal growth on metamorphic buffer layers. He also cofounded Zia Laser, Inc., in 2000, a start-up company with the goal of marketing a new generation of telecommunication and data-communication lasers.

Kevin J. Malloy (SM'77) received the B.S.E.E. degree from the University of Notre Dame, Notre Dame, IN, in 1978 and the Ph.D. degree in electrical engineering from Stanford University, Stanford, CA, in 1984. He served as a program manager at the Air Force Office of Scientific Research from 1983 to 1988. After a term as a Visiting Professor with the University of California, Berkeley, he joined the faculty of the Department of Electrical and Computer Engineering, University of New Mexico (UNM), Albuquerque, as a member of the Center for High Technology Materials. He currently serves as Associate Dean for Research for the School of Engineering at UNM. His research interests include the materials science and physics of semiconductor structures and waves in periodic media.

Peter W. E. Smith (M'67–SM'76–F'78–LF'05) was born in London, U.K., on November 3, 1937. He received the B.Sc. degree in mathematics and physics and the M.Sc. and Ph.D. degrees in physics from McGill University, Montreal, PQ, Canada, in 1958, 1961, and 1964, respectively. His dissertation was on the paramagnetic relaxation of iron group ions in dilute single crystals.

From 1958 to 1959, he was an Engineer with the Canadian Marconi Company, Montreal, where he worked on transistor circuitry. After receiving the Ph.D. degree, he joined Bell Telephone Laboratories, Holmdel, NJ, where he conducted research on laser mode selection and mode-locking, pioneered the development of waveguide gas lasers, and demonstrated and developed hybrid bistable optical devices. In 1970, he spent nine months at the University of California, Berkeley, as a Visiting Mackay Lecturer with the Department of Electrical Engineering, and in 1978–1979 he was a Visiting Research Scientist with the Laboratoire d'Optique Quantique, Ecole Polytechnique, Palaiseau, France. From 1984 to 1992, he was with Bell Communications Research, Red Bank, NJ, where for the last three years he was Division Manager of Photonic Science and Technology Research. In July 1992, he became Professor of Electrical and Computer Engineering, University of Toronto, Toronto, ON, Canada. From 1992 to 1995, he served as Executive Director of the Ontario Laser and Lightwave Research Centre and, from 1999 to 2003, as Director of the Nortel Institute for Telecommunications at the University of Toronto. Since 2003 he has been Professor Emeritus at the University of Toronto and has pursued research interests in photonics involving fiber Bragg grating devices, ultrafast optical switching, and nonlinear optical properties of nanocrystals.

Dr. Smith is a fellow of the Optical Society of America and the Institute of Physics (UK). He is a member of the American Physical Society, and the Canadian Association of Physicists. He has published over 300 technical papers in refereed journals and conference proceedings (with over 6000 citations listed in the ISI Science Citations Index) and holds 34 patents in the photonics area. He has participated in numerous conference organizing committees and has been Guest Editor for several special journal issues. He served as an Associate Editor of the IEEE JOURNAL OF QUANTUM ELECTRONICS from 1976 to 1979, Associate Editor of *Optics Letters* from 1980 to 1982, and Editor of *Optics Letters* from 1991 to 1995. From 1987 to 1991, he served as Editor-in-Chief of the IEEE Press book series *Progress in Lasers and Electro-Optics* and, from 1996 to 1998, as Chair of the Board of Editors of the Optical Society of America. He was the founder of the OSA/IEEE Photonic Switching Conference and served as Co-Chair of the first two conferences in 1987 and 1989. He served as president of the IEEE Lasers and Electro-Optics Society in 1984, and, from 1993 to 1997, was a member of the Board of Directors of the Optical Society of America. He was the recipient of the IEEE Quantum Electronics Award in 1996 and the IEEE Third Millennium Medal in 2000.

J. Stewart Aitchison (M'96–SM'00) received the B.Sc. (with first class honors) and Ph.D. degrees from the Physics Department, Heriot-Watt University, Edinburgh, U.K., in 1984 and 1987, respectively. His dissertation research was on optical bistability in semiconductor waveguides.

From 1988 to 1990, he was a Postdoctoral Member of Technical Staff at Bellcore, Red Bank NJ. His research interests were in high-nonlinearity glasses and spatial optical solitons. He then joined the Department of Electronics and Electrical Engineering, University of Glasgow, Glasgow, U.K., in 1990 and was promoted to a personal chair as Professor of Photonics in 1999. His research was focused on the use of the half-bandgap nonlinearity of III-V semiconductors for the realization of all-optical switching devices and the study of spatial soliton effects. He also worked on the development of quasi-phase-matching techniques in III-V semiconductors, monolithic integration, optical rectification, and planar silica technology. His research group developed novel optical biosensors, waveguide lasers, and photosensitive direct writing processes based around the use of flame-hydrolysis-deposited (FHD) silica. In 1996, he held a Royal Society of Edinburgh Personal Fellowship and carried out research on spatial solitons as a Visiting Researcher at CREOL, University of Central Florida. Since 2001 he has held the Nortel chair in Emerging Technology in the Department of Electrical and Computer Engineering, University of Toronto. His research interests cover all-optical switching and signal processing, optoelectronic integration, and optical bio-sensors. His research has resulted in seven patents, around 185 journal publications, and 200 conference publications. From 2004 to 2007, he was the Director of the Emerging Communications Technology Institute at the University of Toronto. Since 2007, he has been Vice Dean of Research for the Faculty of Applied Science and Engineering, University of Toronto.

Dr. Aitchison is a Fellow of the Optical Society of America and the Institute of Physics, London, U.K.